

Mechanisms of degeneracy breaking in pyrochlore antiferromagnets

Doron L. Bergman¹, Ryuichi Shindou¹, Gregory A. Fiete², and Leon Balents¹

¹*Department of Physics, University of California, Santa Barbara, CA 93106-9530*

²*Kavli Institute for Theoretical Physics, University of California, Santa Barbara, CA 93106-4030*

(Dated: March 23, 2022)

Motivated by the low temperature magnetization curves of several spinel chromites, we theoretically study classical mechanisms of degeneracy lifting in pyrochlore antiferromagnets. Our main focus is on the coupling of spin exchange to lattice distortions. Prior work by Penc et al. (Phys. Rev. Lett. 93, 197203 (2004)) has demonstrated that such coupling leads to a robust magnetization plateau at half the saturation moment per spin, in agreement with experiment. We show that a simple Einstein model incorporating local site distortions generates a “universal” magnetic order on the plateau, and highlight the distinct predictions of this model from that in Penc et al. (Phys. Rev. Lett. 93, 197203 (2004)). We also consider the complementary degeneracy-lifting effects of further neighbor exchange interactions. We discuss the implications for transitions off the plateau at both the high field and low field end, as well as at fields close to the saturation value. We predict that under certain circumstances there is spontaneous *uniform* XY magnetization (transverse to the field) for field values just above the plateau. These features may be tested in experiments. While selecting a unique magnetic order in the half magnetization plateau, at zero magnetic field the Einstein model retains an extensive degeneracy, though significantly reduced compared with the pure Heisenberg antiferromagnet.

PACS numbers: 75.10.-b,75.10.Jm,75.25.+z

I. INTRODUCTION

The pyrochlore lattice with nearest-neighbor antiferromagnetically coupled spins is well-known as one of the most frustrated and degenerate magnetic systems.^{2,3} Ultimately, this degeneracy must be lifted at low temperature, but the mechanisms responsible can vary greatly from material to material and also depend on applied fields, pressure, and other variables. In this paper we focus primarily on how degeneracies present at finite magnetic fields are lifted by the coupling of spin and lattice degrees of freedom.

Recent experiments on a number of insulating chromite compounds, namely ZnCr_2O_4 , CdCr_2O_4 and HgCr_2O_4 have revealed distinctive common features in their low-temperature magnetization curves^{4,5} and other interesting properties in neutron scattering.^{6,7} At low magnetic fields the magnetization curve grows linearly with magnetic field. At one point there is a sharp jump in magnetization onto a rather robust plateau, with half the full magnetization per spin. In HgCr_2O_4 it is possible at yet higher fields to observe a smooth transition off of the half-magnetization plateau, and a gradual increase in magnetization up to what may be a fully polarized plateau state.⁴

The Cr^{+3} ions sit at the center of octahedra of O^{-2} ions, and thus the outer d-orbital electron shell undergoes crystal field splitting to a lower energy t_{2g} orbital triplet, and a higher energy e_g orbital doublet. The t_{2g} orbitals hold 3 electrons, and therefore by Hund’s rule form a spin $\frac{3}{2}$ degree of freedom, with no orbital degeneracy (therefore the cooperative Jahn–Teller effect cannot lift the degeneracy in this system). These spins are the source of magnetic behavior in these compounds. The

Cr^{+3} ions sit on the sites of a pyrochlore lattice, and therefore a minimal model for the magnetic properties of these compounds is the nearest-neighbor Heisenberg anti-ferromagnet, with the Hamiltonian

$$\mathcal{H} = J \sum_{\langle ij \rangle} \mathbf{S}_i \cdot \mathbf{S}_j - \mathbf{H} \cdot \sum_j \mathbf{S}_j . \quad (1)$$

Here \mathbf{H} is proportional to the applied magnetic (Zeeman) field. In this paper, we will treat the spins as classical, and simplify notation by normalizing them as unit vectors (absorbing a factor of S^2 into J). Much previous work has been devoted to this and similar models in zero magnetic field.^{8,9,10,11,12,13,14} A useful rewriting of the Hamiltonian is

$$\mathcal{H} = \frac{J}{2} \sum_t [(\mathbf{S}_t - \mathbf{h})^2 - \mathbf{h}^2] , \quad (2)$$

where $\mathbf{S}_t = \sum_{j \in t} \mathbf{S}_j$ is the sum of spins on a tetrahedron labeled by t , $\mathbf{h} = \mathbf{H}/2J = h\hat{z}$ and we have ignored a trivial constant term in the Hamiltonian. This model has a macroscopically degenerate classical ground state manifold at all fields up to full polarization: any state with $\mathbf{S}_t = \mathbf{h}$ on all tetrahedra is a classical ground state.

Within this (over-)simplified picture, the magnetization is everywhere a smooth (linear at low temperatures, since the magnetization is proportional to the average \mathbf{S}_t) function of the field, and there are no plateaus. Instead, some other effects or interactions must be considered to explain the observed plateau. On general grounds, a plateau is expected to be associated with some breaking of degeneracy, into a state in which the spontaneous static moments of the spins are all parallel or antiparallel to the field axis. Quantum mechanically, this is simply

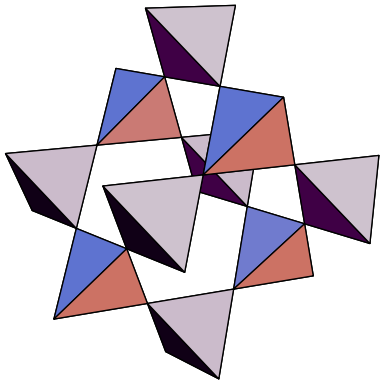


FIG. 1: The pyrochlore lattice. A network of corner sharing tetrahedra.

because, in a non-collinear *ordered* state, the Goldstone theorem associated with $U(1)$ symmetry-breaking around the applied field direction ensures the presence of a gapless magnetic excitation (spin wave), which contradicts the incompressibility of the magnetization plateau. The analogous classical argument is that a non-collinear spin state may always be arbitrarily slightly deformed to lower its free energy in response to a change in field, which by thermodynamics implies a non-constant magnetization. Hence, to understand the plateau, we seek mechanisms to select one or a set of collinear ground states out of the classically degenerate manifold. On the pyrochlore lattice, the natural collinear states for the half-polarized plateau^{5,15,16} are those with 3 “majority” spins aligned parallel to the magnetic field, and 1 “minority” spin aligned antiparallel to the field, *on each tetrahedron*. However, even if one assumes a collinear state for the spins, a massive degeneracy of the ground state still remains, since there is considerable freedom in fixing the location of the minority spin on each tetrahedron.

The possibility that quantum fluctuations might control the state selection – of and within the collinear 3:1 manifold – has been explored elsewhere.^{15,16,17} Here we will investigate alternative mechanisms, within classical models.¹⁸ A guide to the possible physical processes involved comes from two sets of observations. First, it has been noted experimentally that the above chromite materials, ACr_2O_4 , exhibit strong magnetostriction, especially upon entering the plateau region.^{4,5} This strongly suggests that spin-lattice coupling plays an important role in the plateau formation. Second, studies of the structurally and electronically analogous set of spinels, $\text{ACr}_2(\text{S,Se})_4$ – with S or Se replacing O atoms and the same non-magnetic A atoms – display *ferromagnetic* tendencies or long-range order, and in some cases an apparent competition of ferromagnetic and antiferromagnetic interactions.¹⁹ This indicates drastic changes in the magnetic interactions may be effected by small changes in

structural parameters. More specific implications of the trends in these materials for the chromites will be discussed later.

This main analysis and results of this paper are as follows. Guided by the above observations, we focus primarily on a *minimal* model for the plateau structure involving *only* spin-lattice coupling. In this minimal model, the lattice modes are taken into account by the simplest possible Einstein phonons describing motions of the magnetic sites. We show that this model indeed captures a simple and robust mechanism for plateau formation *and* predicts a unique ordered 3:1 state – the “R” state, shown in Fig.4 – on the plateau. Extended to the full range of magnetic fields, this Einstein model predicts a first-order transition to a non-collinear ground state at lower fields below the plateau, and a second-order transition to a *canted ferrimagnetic* state above the plateau. The canted ferrimagnet retains the Ising order of the R state, but in addition possesses XY *ferrimagnetic* order of the magnetic moments transverse to the field axis. At zero field, the Einstein model retains a large ground state degeneracy, though it is still vastly reduced from that of the ideal model without spin-lattice coupling.

A plateau with the same R state structure can also be stabilized by a *combination* of spin-lattice and further-neighbor exchange interactions. We give the conditions on these further-neighbor exchanges for this to occur. Consistency of this more complicated but still feasible scenario could be then tested by placing independent constraints on these couplings from other measurements. This is considered further in the Discussion.

A number of studies of spin-lattice and further-neighbor exchange effects in pyrochlores have already been carried out. A well-known analysis of certain zero field spin-lattice couplings by Tchernyshyov *et al.* christened the resulting degeneracy-breaking a “spin Jahn Teller” effect.²⁰ Because this analysis was at zero field, and because it considered only $q = 0$ phonons, it has little bearing on the present work. More relevant is the pioneering study of spin-lattice couplings on the plateau by Penc *et al.*¹ Their work provides a simple explanation of the plateau formation, but unlike the theory in this paper, does not explain the breaking of degeneracy within the 3:1 states. We will compare their “bond phonon” Hamiltonian with our Einstein model throughout this paper.

The remainder of this paper is organized as follows. In Sec. II we present two models of spin-lattice coupling, a “bond” model and a “site” model. In Sec. III we discuss the implications of these two models for the magnetic order on the half-saturation magnetization plateau and the transition off the high and low field edges of the plateau. We discuss a more general model with further neighbor spin interactions in Sec. IV. Finally, a discussion of our main results and their relevance to experiment is given in Sec. V.

II. SPIN-LATTICE COUPLING

In this section we discuss some simple models for the coupling of the magnetic degrees of freedom to phonon modes. We will treat the spins and phonons classically and in equilibrium. With these assumptions, the statistical mechanics of the phonons is captured by a Gaussian integral over the associated set of displacement coordinates in the partition function. In such a case, the phonons can (if desired) be integrated out to obtain an effective spin Hamiltonian which contains additional interactions beyond the Heisenberg form.

Let us first make a few general comments regarding spin-lattice interactions. For a fixed, static, distortion of the lattice, we expect modifications of the exchange interactions that are (to an excellent approximation) linear in the displacement coordinates. Neglecting weak spin-orbit effects, the exchanges remain of Heisenberg form.¹⁸ Therefore the general form of the modified exchange is

$$\mathcal{H}_{\text{ex}} = J \sum_{\langle ij \rangle} \mathbf{S}_i \cdot \mathbf{S}_j [1 - \gamma u_{ij}], \quad (3)$$

where u_{ij} is the linear combination of displacement coordinates coupled to the pair of spins i, j . Because all nearest-neighbor pairs of pyrochlore sites are equivalent, they are all described by a single spin-lattice constant γ .

A naïve interpretation of Eq. (3) is that u_{ij} is proportional to the *distance* between spins i and j . As the distance is increased/decreased, the overlap between electronic wavefunctions on the two sites decreases/increases, leading to a change in the exchange coupling, proportional to this distance. This picture is in fact appropriate for *direct exchange*, in which there is no intervening oxygen as in superexchange. In the spinel chromites, the antiferromagnetic Cr-Cr is indeed believed to arise from direct exchange.²¹ More generally, the dependence of exchange on displacements may involve changes in the bond angles as well as distances. Nevertheless, from this simplistic view, one expects $\gamma > 0$ (hence the minus sign in Eq.(3)), and γ of order the inverse of the effective Bohr radius of the electronic orbitals involved.

A. Bond phonon model

In the model of Penc *et al.*,^{1,22} the u_{ij} are taken as independent parameters, i.e. the length of each pyrochlore bond can independently expand or contract. This “bond phonon” (BP) model has the elastic energy

$$\mathcal{H}_{\text{ph}}^{BP} = \frac{k_{BP}}{2} \sum_{\langle ij \rangle} u_{ij}^2, \quad (4)$$

where k_{BP} is an elastic constant. Because each u_{ij} couples only to a single nearest-neighbor pair of spins, and in this model each u_{ij} is independent, the spin-lattice interaction does not induce any effective interactions amongst

further neighbor spins. Instead, integrating out the u_{ij} according to

$$e^{-\beta \mathcal{H}_{\text{eff}}^{BP}[\{\mathbf{S}_i\}]} = \prod_{\langle ij \rangle} \int du_{ij} e^{-\beta(\mathcal{H}_{\text{ex}}[\{\mathbf{S}_i, u_{ij}\}] + \mathcal{H}_{\text{ph}}^{BP}[\{u_{ij}\}])}, \quad (5)$$

one obtains, up to a constant, an effective spin Hamiltonian of the form

$$\mathcal{H}_{\text{eff}}^{BP} = J \sum_{\langle ij \rangle} [\mathbf{S}_i \cdot \mathbf{S}_j - b(\mathbf{S}_i \cdot \mathbf{S}_j)^2]. \quad (6)$$

Thus, in this BP model, the spin-lattice coupling induces an effective bi-quadratic interaction or relative strength $b = \frac{\gamma^2 J}{k_{BP}}$ between nearest-neighbor spins. Note that this term favors configurations in which neighboring spins are either parallel or antiparallel, i.e. collinear configurations. The BP model therefore gives a simple explanation for the preference for 3:1 states in the field range in which the classical Heisenberg model prefers half-magnetization states.^{15,16}

The preference for collinear spin arrangements can be understood physically in terms of the phonons as follows. If a given pair of spins is antiferromagnetically aligned, then the spin-lattice coupling in Eq.(3) can be made most negative by choosing $u_{ij} < 0$, i.e. contracting the bond to enhance the effective exchange. Conversely, if a pair of spins is ferromagnetically aligned, the bond can expand ($u_{ij} > 0$) to weaken the ferromagnetic exchange interaction. In either case, the bond energy is lowered by the same amount (because of the linear phonon coupling) relative to the undistorted bond.

It is straightforward to see that, as claimed earlier, all the 3:1 plateau configurations remain degenerate within the BP model. By rewriting the exchange interaction as in Eq. (2), one obtains

$$\mathcal{H}_{\text{eff}}^{BP} = \frac{J}{2} \sum_t [(\mathbf{S}_t - \mathbf{h})^2 - \mathbf{h}^2] - bJ \sum_{\langle ij \rangle} (\mathbf{S}_i \cdot \mathbf{S}_j)^2. \quad (7)$$

For $h = 2$, every 3:1 configuration minimizes the first term on each tetrahedron as well as the second term on each link. Hence they are the global ground states and all degenerate. Furthermore, even for different values of h , all these states remain degenerate, since they have the same (no longer minimal in exchange energy) \mathbf{S}_t on each tetrahedron, and the same (minimum in energy) value of the bi-quadratic term. We will return to discuss the magnetization curve and configurations away from the plateau in Sec III.

B. Einstein (site) phonon model

The lack of splitting of the degeneracy of the 3:1 states is a non-generic feature of the BP model. It arises from the fact that the bond displacements are taken to be completely independent of one another, so that they can

induce no spin correlations beyond nearest-neighbor. In reality, however, this is not the case. To make a change in a given bond length requires moving one or both of the atoms involved, which will at least distort the other bonds connected to these atoms. A more natural phonon model can be formulated in terms of the independent displacements of each *atom*, with the bond distances determined from these atomic displacements. If the harmonic phonon energy is taken to be a sum of independent restoring forces for each atom, this is simply the conventional Einstein model. As usual, such an Einstein model provides a crude but reasonable approximation, provided the most important phonons are optical phonons rather than the long-wavelength $q \approx 0$ acoustic modes.

We therefore adopt this Einstein (site rather than bond) phonon model. To derive an appropriate form, let us assume a distance dependent exchange coupling (see e.g. Ref. 18 in a zero field context). It can be expanded in small atomic displacements \mathbf{u}_i for each site i :

$$\begin{aligned} J_{ij} &\equiv J(|\mathbf{r}_i - \mathbf{r}_j|) \approx J(\mathbf{R}) + (\mathbf{u}_i - \mathbf{u}_j) \cdot \nabla J(\mathbf{R}) + \dots \\ &\approx (1 - \gamma \mathbf{e}_{ij} \cdot (\mathbf{u}_i - \mathbf{u}_j)) J, \end{aligned} \quad (8)$$

where \mathbf{R} is the vector between the pyrochlore sites i and j , and $\mathbf{e}_{ij} = \mathbf{R}/|\mathbf{R}|$ is the unit vector in the corresponding equilibrium direction. Comparing to Eq.(3), the Einstein model has then

$$u_{ij} = \mathbf{e}_{ij} \cdot (\mathbf{u}_i - \mathbf{u}_j), \quad (9)$$

with the elastic energy given by

$$\mathcal{H}_{\text{ph}}^E = \frac{k_E}{2} \sum_i |\mathbf{u}_i|^2. \quad (10)$$

It is amusing to note that although the independent modes considered are quite distinct in the bond and site phonon models, on the pyrochlore lattice both formulations contain the same number of degrees of freedom. The site displacement vectors represent 3 degrees of freedom for each site, which for N sites of the pyrochlore lattice gives a total of $3N$ degrees of freedom. On the other hand, there are 6 links per tetrahedra, and one scalar bond phonon per link. There are $N/2$ tetrahedra in the lattice, so the total number of degrees of freedom in the bond phonon model is also $3N$.

Just as we did for the BP model, we now proceed to integrate out the site Einstein phonons. Because the Hamiltonian is quadratic in the displacements, this Gaussian integration is equivalent to simply minimizing the Hamiltonian with respect to the set of \mathbf{u}_i and eliminating these in favor of the spin variables. The optimal values of the displacements are simply

$$\mathbf{u}_j^* = -\frac{J\gamma}{k_E} \sum_{i \in N(j)} (\mathbf{S}_i \cdot \mathbf{S}_j) \mathbf{e}_{ij}, \quad (11)$$

where $N(j)$ denotes the set of nearest neighbors of site j . At this point, it is evident already that the presence of

lattice distortions is tied to frustration. If all exchanges could be satisfied equally, i.e. $\langle \mathbf{S}_i \cdot \mathbf{S}_j \rangle = \text{const}$, then the distortion vanishes: $\langle \mathbf{u}_j^* \rangle \sim \sum_{i \in N(j)} \mathbf{e}_{ij} = 0$. A distorted lattice is thus induced only in frustrated states, and for instance no distortion is expected at large fields where the spins are fully and uniformly polarized. If a distortion is still observed in a fully polarized state, it cannot arise from this mechanism, and might have no connection with the magnetic order of the system.

Substituting back Eq.(11) in the Hamiltonian, we obtain the effective Hamiltonian for the (site) Einstein (E) model:

$$\mathcal{H}_{\text{eff}}^E = J \sum_{\langle ij \rangle} \mathbf{S}_i \cdot \mathbf{S}_j - \frac{k_E}{2} \sum_j |\mathbf{u}_j^*|^2, \quad (12)$$

where, as above, the Zeeman interaction with the external field has been dropped for brevity. The form in Eq.(12) is actually quite convenient for analysis, but we first write out the induced interactions explicitly for comparison with the BP model. One finds

$$\begin{aligned} \mathcal{H}_{\text{eff}}^E &= J \sum_{\langle ij \rangle} [\mathbf{S}_i \cdot \mathbf{S}_j - b (\mathbf{S}_i \cdot \mathbf{S}_j)^2] \\ &\quad - J \frac{b'}{2} \sum_{j \neq k \in N(i)} (\mathbf{S}_i \cdot \mathbf{S}_j) (\mathbf{S}_i \cdot \mathbf{S}_k) \mathbf{e}_{ij} \cdot \mathbf{e}_{ik}, \end{aligned} \quad (13)$$

with $b = \frac{J\gamma^2}{k_E}$ as before. Here we have defined a separate parameter b' which, according to the strict development above, is not independent ($b' = b$). However, it distinguishes the additional terms in the effective spin Hamiltonian which are not present in the BP model. We propose to view b' as a separate phenomenological parameter to describe the phonon modes. In particular, taking $0 < b' < b$ corresponds to ‘‘softening’’ the bond phonons somewhat, and interpolating between the Einstein model and the BP model.

Because the same biquadratic term is present as in the BP model, we may expect that, as in that case, collinear states are favored. Indeed, when the additional terms are weak, $b' \ll b$, they may be viewed as weak perturbations. Since the b term already selects collinear 3:1 configurations, the $b' > 0$ term can then only select a ground state within this set of states, and has little effect on the stability of the plateau. We show below that $b' > 0$ selects a particular collinear classical spin configuration depicted in Fig.4, in the manifold of 3:1 states. Our analysis shows that for the range of parameters $b' (< \frac{b}{2})$ the plateau retains a finite width, and the same particular 3:1 configuration prevails.

To get some intuition for how additional degeneracy-breaking is induced by the b' terms, assume a collinear state, $\mathbf{S}_i = \hat{\mathbf{z}}\sigma_i$, with $\sigma_i = \pm 1$ Ising spins satisfying the 3:1 constraint. The first line in Eq.(13) becomes constant, and the four-spin product $(\mathbf{S}_i \cdot \mathbf{S}_j)(\mathbf{S}_i \cdot \mathbf{S}_k) = \sigma_j \sigma_k$ becomes an effective two-spin interaction. Then the

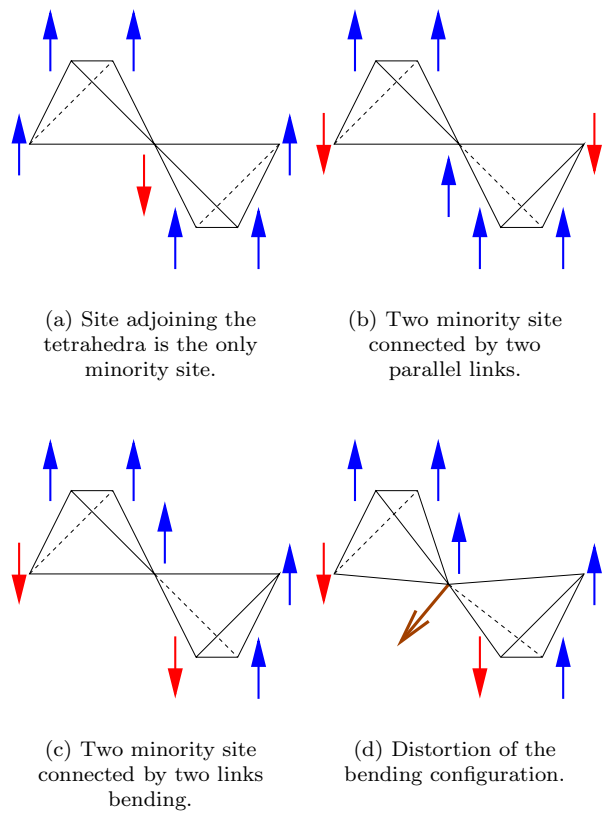


FIG. 2: (Color online) The three generic configurations of minority sites (red arrow) on two adjacent tetrahedra.

Hamiltonian within the 3:1 manifold takes the form of Ising exchange terms:

$$\mathcal{H}_{3:1}^E = J_2^{\text{eff}} \sum_{\langle\langle ij \rangle\rangle} \sigma_i \sigma_j + J_3^{\text{eff}} \sum_{\langle\langle kl \rangle\rangle} \sigma_k \sigma_l, \quad (14)$$

where we have dropped some terms which are constant in the 3:1 manifold. The parameters $J_2^{\text{eff}} = Jb'/4$ and $J_3^{\text{eff}} = Jb'/2$ are the effective Ising exchanges between second-neighbor sites (connected by two bent links as in Fig.2(c)) and third-neighbor sites (connected by two parallel links as in Fig.2(b), and explicitly shown in Fig. 3). Note that J_3^{eff} is twice as large as J_2^{eff} , so the third neighbor interactions tend to be favored over second neighbor interactions in the determination of the magnetic state.

Clearly these effective interactions break the degeneracy of the 3:1 manifold. To understand this breaking more physically, and thereby derive the selected ordered state on the plateau, we return to the formulation of Eq.(12). From Eq.(12) it is readily apparent that the larger the induced lattice displacement, the lower the energy. For $b \ll 1$, we may assume half-magnetization on each tetrahedron in the plateau region, and then consider the effect of the lattice displacement as a perturbation.

Let us begin by first assuming the 3:1 constraint on each tetrahedron. We then wish to understand which

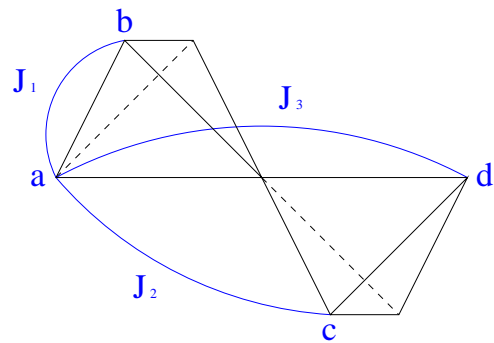


FIG. 3: (Color Online) Further neighbor interactions in the pyrochlore lattice. The nearest neighbor interaction J_1 is between site a and site b , the next nearest neighbor interaction J_2 is between site a and site c , and finally the next next nearest neighbor interaction J_3 is between site a and site d .

configurations of minority spins maximize the displacements. Consider 2 tetrahedra adjoined by a site j . There are 3 generic configurations of the positions of the minority sites, depicted in Fig. 2. A *fixed* fraction (1/4) of all configurations are necessarily those in Fig.2(a), therefore the energy of this configuration is irrelevant to the splitting. Of the remaining two configurations, it is simple to understand that a nonzero \mathbf{u}_j^* can only arise in the configuration Fig. 2(c), because it is the only configuration with asymmetry about the site j . Therefore, we wish to maximize the number of configurations of this type.

We can describe this favored configuration with a “bending rule”. For every pair of adjacent tetrahedra adjoined by a majority site, mark the links connecting between the two minority sites. These marked links form paths on the lattice, connecting all the minority sites. It is energetically preferable for these these paths to bend, rather than continue on a straight line. Clearly, the maximum number of such bent paths is obtained if *all* paths are bent, i.e. all minority sites are in the configurations in Fig.2(c). This can indeed be achieved. By careful enumeration of all configurations (see appendix B for details), it can be shown that there is a unique (up to lattice symmetries) configuration which satisfies this “bending rule” on a “pyrochlore cell” – a volume containing 4 hexagonal plaquettes (see Fig. 4). If this configuration is required on all such cells, the ground state is completely specified. This is precisely the “R” state obtained in Ref. 15 in a very different quantum dimer model analysis. The “R” state has space group $P4_332$ and may be thought of in terms of filling the pyrochlore lattice with a fraction 1/4 of hexagonal plaquettes with alternating up/down spins and a fraction 3/4 of plaquettes with one down spin and five up spins.

Because the argument above proves the R-state is the best possible collinear state, any alternative ground state must be non-collinear. Since non-collinear states cannot exhibit a plateau, proving that the R-state is the global minimum energy state is equivalent to proving the existence of a plateau. However, it is important to emphasize

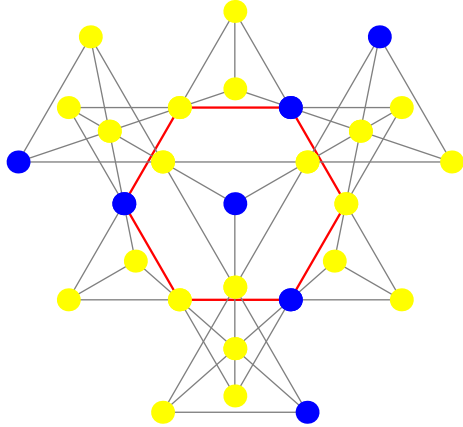


FIG. 4: (Color online) Spin configuration of the R state. Majority sites are colored yellow, minority sites are colored blue. The flippable plaquette in this unit cell of the R-state configuration is highlighted in red.

that the above argument assumes the 3:1 configurations (actually it can be made equally rigorous assuming only collinearity). For $b' \ll b$, this assumption is valid, and the above argument becomes controlled. For the generic situation with $b' \sim b$, the effective Hamiltonian is actually “frustrated” in the following sense. Because the Einstein phonon displacement resides on a pyrochlore site and is related via Eq.(11) to spins on the two neighboring tetrahedra, the natural unit for the effective Hamiltonian is no longer a bond but such a pair of adjacent tetrahedra. One may rewrite the Hamiltonian as a sum over such pairs, parametrized by the pyrochlore site j they share: $\mathcal{H} = \sum_j \mathcal{H}_j$, with

$$\begin{aligned} \mathcal{H}_j = & \frac{J}{8} [(\mathbf{S}_{t_1} - \mathbf{h})^2 - h^2] + \frac{J}{8} [(\mathbf{S}_{t_2} - \mathbf{h})^2 - h^2] \\ & - J \frac{b}{4} \sum_{\langle ik \rangle \in t_{1,2}} (\mathbf{S}_i \cdot \mathbf{S}_k)^2 \\ & - J \frac{b'}{2} \sum_{i \neq k \in N(j)} (\mathbf{S}_i \cdot \mathbf{S}_j)(\mathbf{S}_j \cdot \mathbf{S}_k) \mathbf{e}_{ji} \cdot \mathbf{e}_{jk} . \end{aligned} \quad (15)$$

The extra factors of $\frac{1}{4}$ above relative to Eq.(2) in the nearest neighbor terms are due to the fact that every tetrahedron is shared by 4 pyrochlore sites. One can show that for $b, b' > 0$, for a non-zero window of fields h in the neighborhood of $h = 2$ (the plateau region), \mathcal{H}_j

is minimized, when the pair of adjacent tetrahedra sharing site j is in the “bending” configuration pictured in Fig.2(c). Clearly, however, this condition cannot be *simultaneously* satisfied on every tetrahedral pair, because some of the tetrahedron pairs must have a minority site adjoining them. Thus the Einstein site phonon model exhibits “tetrahedral-pair frustration”. The R-state argued for above resolves this frustration in a natural way, by minimizing the energy on a maximal fraction of tetrahedral pairs (which is $3/4$). Because such a relatively large fraction of tetrahedron pair units are “satisfied”, it appears plausible that the R-state is indeed the global ground state.

We have searched numerically to check for the alternative possibility, that a lesser fraction (perhaps zero) of units are satisfied, but that the energy of the dis-satisfied units is sufficiently better as to lower the total energy. In order to take the “tetrahedral-pair frustration” into account, we must go beyond the above single-tetrahedron analysis for the BP model. In particular, we must consider units larger than a single tetrahedron, and also larger than a single tetrahedron-pair unit: since these units are frustrated, they cannot be simultaneously satisfied at most fields. Instead, we consider a cluster of five tetrahedra consisting of a central tetrahedron and its four surrounding neighbors. This is the smallest collection of tetrahedra for the 3:1 states in which a pair in the unsatisfied configuration of Fig. 2(a) *must* appear. The Hamiltonian can be written as a sum over the up pointing tetrahedra $\mathcal{H} = \sum_{t \in \uparrow} \mathcal{H}_t$, t being the central tetrahedron in each cluster. The down pointing tetrahedra are counted in 4 different clusters in this scheme, so we account for this by writing the cluster Hamiltonian as

$$\begin{aligned} \mathcal{H}_t = & \frac{J}{2} [(\mathbf{S}_{t_0} - \mathbf{h})^2 - h^2] + \frac{J}{8} [(\mathbf{S}_{t_1} - \mathbf{h})^2 - h^2] \\ & + \frac{J}{8} [(\mathbf{S}_{t_2} - \mathbf{h})^2 - h^2] + \frac{J}{8} [(\mathbf{S}_{t_3} - \mathbf{h})^2 - h^2] \\ & + \frac{J}{8} [(\mathbf{S}_{t_4} - \mathbf{h})^2 - h^2] - J \frac{b}{4} \sum_{\langle ik \rangle \in t_{0,1,2,3,4}} (\mathbf{S}_i \cdot \mathbf{S}_k)^2 \\ & - J \frac{b'}{2} \sum_{j=1}^4 \sum_{i \neq k \in N(j)} (\mathbf{S}_i \cdot \mathbf{S}_j)(\mathbf{S}_j \cdot \mathbf{S}_k) \mathbf{e}_{ji} \cdot \mathbf{e}_{jk} , \end{aligned} \quad (16)$$

where t_0 is the middle tetrahedron, $t_{1..4}$ are the other four tetrahedra, and the sites $j = 1..4$ are the 4 corners of the tetrahedron t_0 .

The conclusion from our numerical study, is that for $0 < b' \lesssim b/2$, the minimum of \mathcal{H}_t above is indeed a 3:1 configuration comprising a corresponding section of the R-state. Hence, because such a configuration can be simultaneously realized on every such unit, in this parameter range, the spin-lattice coupling indeed stabilizes a state with the R-state symmetry. The width of the corresponding plateau is discussed in the following section.

III. AWAY FROM HALF-POLARIZATION

In this section, we explore the properties away from the magnetization plateau.

A. BP Model

Let us first review the findings of Penc *et al*¹ in the BP model. The basic results can be understood by simple considerations on a single tetrahedron. Such a simplification is satisfactory in this case because the Hamiltonian can be written as a sum of such terms on each tetrahedron, and they can be simultaneously satisfied. Thus the BP model does not suffer from “tetrahedral-pair frustration”.

For magnetization greater than half polarization, the ground state has a 3:1 configuration, with 3 majority spins and 1 minority spin on each tetrahedron. However, they are not collinear, except on the plateau and at saturation. These vary in such a way that the net spin per tetrahedron is increased from 2, by *smoothly* rotating the minority spin from down to up. Because the collinear plateau state can be smoothly deformed into the states above the plateau, there is a *continuous* transition at the upper plateau edge.¹ All these states above the plateau share the same degeneracy as the plateau states: the location of the minority spins is not determined in the BP model.

On the other hand, a state with magnetization per tetrahedron of less than 2 cannot be achieved with a 3:1 configuration. Thus, for fields below the plateau, the structure of the configurations *must* change. Instead, over most of this region of phase space, the spin configuration assumes a 2:2 form. This implies a discontinuous change of spins, and gives rise to a *first order* transition.¹ Like the 3:1 states, these 2:2 states are highly degenerate, due to the many equivalent manners in which each of the 2 spin polarizations may be arranged. Both above and below the plateau, the low temperature phases break rotational symmetry about the field axis, but with no net moment in the $x - y$ plane.

B. Einstein model

1. Magnetization

The BP model captures rather well the broad behavior of the low-temperature magnetization curve, $M(H)$, in the chromites, where it has been observed. The only qualitative exception is the observation of a small feature at $H \approx 37T$ for HgCr_2O_4 , in the field range between the plateau and saturation, which has been suggested as an additional phase transition.⁴

The magnetization curves we obtained for the Einstein model ($b' < b$) are similar to those for the BP model over most field values. Studying the magnetization curve for

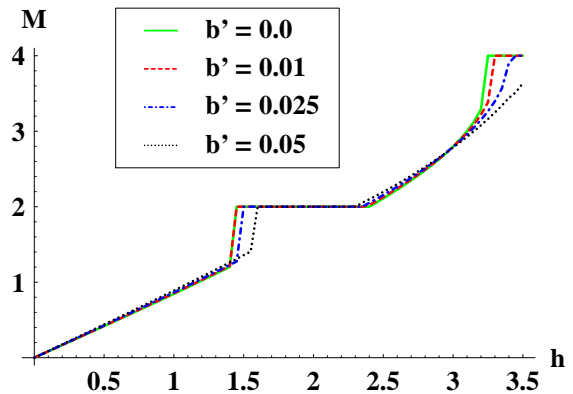


FIG. 5: (Color online) Magnetization curves for various values of b' with $b = 0.1$ fixed, where b and b' are given below Eq.(15). The plateau width decreases with growing b' .

the Einstein model, however, is much more involved than the above single-tetrahedron analysis for the BP model, due to the “tetrahedral-pair frustration”, explained in the previous section. Following the above treatment, we consider a collection of five tetrahedra. On this cluster, we numerically minimize the energy (16) for each field, and determine the zero-temperature $M(H)$ curve for given values of b, b' . The magnetization curves for one value of $b = 0.1$ and various values of b' are plotted in Fig. 5.

In the magnetization curve shown in Fig. 5 an abrupt jump is observed going from the linear regime into the half magnetization plateau region, in accordance with the results of Penc *et al*.¹ Given the 2:2 spin configuration at zero magnetic field, and the 3:1 configuration in the plateau region, we can contemplate a sharp transition onto the plateau between 2:2 and 3:1 configurations. Such a transition would have to be first order, as the symmetry groups are not Landau-Ginzburg compatible for a second order transition (one is not the subgroup of the other).

2. Phases

As we have seen above, the differences in the magnetization curves of the Einstein and BP models are minimal. The magnetization, as a purely thermodynamic quantity, is only weakly sensitive to the detailed correlations between spins beyond one or two lattice spacings. A better test of the differences between the models is to compare their phase diagrams. In the BP model, as described above, there are four “phases”, in which the local structures on each tetrahedra are distinct: at low fields, a 2:2 structure or a “splayed” structure; on the plateau, a collinear 3:1 structure; above the plateau, a non-collinear 3:1 structure, and at high fields, the ferromagnetic fully saturated configuration.¹ We have used quotation marks around the word “phases” because all but the ferromagnetic configuration exhibit an unphysi-

Number of unit cells	Number of bending ice configurations
$2 \times 2 \times 2 = 8$	12
$2 \times 2 \times 4 = 16$	36
$2 \times 4 \times 4 = 32$	82
$4 \times 4 \times 4 = 64$	216

TABLE I: Bending Ice configurations. Dimensions of pyrochlore cluster indicated. Periodic boundary conditions were used.

Number of unit cells	Number of ice configurations
$2 \times 2 \times 1 = 4$	78
$3 \times 2 \times 1 = 6$	534
$2 \times 2 \times 2 = 8$	2970
$3 \times 3 \times 1 = 9$	7974
$5 \times 2 \times 1 = 10$	28326
$3 \times 2 \times 2 = 12$	87684

TABLE II: Ice configurations. Dimensions of pyrochlore cluster indicated. Periodic boundary conditions were used.

cal macroscopic degeneracy not related to symmetry.

A full determination of the phase diagram in the Einstein model is beyond the scope of this paper. However, we will outline those features which are similar and those which are clearly distinguishable from the BP model. At zero field, it can be shown that the ground states of the Einstein model are far less degenerate for all $b' > 0$ than those of the BP model. To see this, we use the representation in Eq.(15), and consider the minimum energy configuration on a single tetrahedral-pair with $h = 0$. Simple analysis shows that this minimum energy occurs for collinear states with a 2:2 ratio of “up” and “down” spins on each of the two tetrahedra, satisfying the “bending rule” if links are drawn between the spins aligned with the central one. Because the field $h = 0$, the spin axis is arbitrary. Unlike in the plateau region, such 2:2 states are *unfrustrated*: every tetrahedral pair can be chosen to have such a configuration. In fact, these states are still highly degenerate. They correspond to “ice-rules” states, with the additional constraint of the “bending rule”. Though we do not have an analytical calculation of the number of such states, we have performed a numerical enumeration of them on various finite size clusters (see Table I). Evidently, the number of such “bending ice” states grows rapidly with system size. It is likely that these states are macroscopically degenerate. Nevertheless, this set of states is much less degenerate than the zero field ground states in the BP model, which are simply *all* the 2:2 “ice” states, without the bending rule imposed (see Table II). We will comment upon the physical consequences of this degeneracy in Sec. V.

At small non-zero fields, we expect the same “bending rule” states to remain approximate ground states, with the axis of the two spin orientations “flopped” into a fixed one at a small angle (proportional to h/J) away from the

$x - y$ plane in spin space. Thus in this region there is a broken XY symmetry around the spin-rotation axis. Indeed numerical minimization of a tetrahedron pair shows that for finite weak magnetic field the nearly collinear 2:2 bending state persists. For intermediate fields half-way between zero field and the plateau, we do not have definitive results. As in the BP model, there is a first order transition separating the low-field region from the plateau.

Like in the BP model, at fields just above the plateau, the 3:1 structure deforms smoothly into a state with larger than half polarization by small rotations of the spins. Because this deformation is smooth, we expect that the space group symmetry of the “canted ferrimagnetic” state just above the plateau will be *at least as low* as the $P4_332$ symmetry of the R-state. This should be observable in neutron scattering as the persistence of magnetic scattering peaks – present in $P4_332$ but not the $Fd\bar{3}m$ space group of the ideal spinel – in the field region above the plateau. This is a distinct prediction of the Einstein model.

In addition to this persistent discrete symmetry breaking, this region also exhibits XY long range order of the spin components perpendicular to the field. The nature of this XY order is not apparent from simple arguments. Classically, it can be analyzed for the Einstein model by assuming small deformations of the spins,

$$\mathbf{S}_i = \left(\text{Re}\psi_i, \text{Im}\psi_i, \sigma_i \sqrt{1 - |\psi_i|^2} \right), \quad (17)$$

where $\sigma_i = \pm 1$ is the Ising magnetization of spin i in the R-state, and ψ_i is the transverse spin represented as a complex vector. By inserting this into Eq.(13) and expanding to quadratic order, one obtains a quadratic form in ψ_i . This can be diagonalized using Bloch’s theorem to obtain a set of 16 (one per site of the R-state unit cell) “bands”. The first vanishing eigenvalue(s) of this spectrum on increasing field signals the upper edge of the plateau. The eigenfunction (wavevector(s) and wavefunctions) is the order parameter of the XY magnetism in the canted ferrimagnet.

We have carried out this calculation for $b = 0.1$ and $b' = 0.0, 0.01, 0.025, 0.05$ (the same values for which we plotted the magnetization curve in Fig. 5), and a range of magnetic fields sweeping through the transition off the plateau. Our findings are that the excitation minimum is at $\mathbf{k} = 0$ (the Γ point), with an eigenfunction which retains all the point group symmetries of the R-state. The resulting non-vanishing XY components of the spins just above the plateau are equal on all minority sites and equal on all majority sites. However, their direction is opposite on the two types of sites, and the magnitude of the transverse component on the minority sites is always larger than that of the majority sites, by a factor which is very close but not precisely equal to 3. This indicates that there is a *non-vanishing total XY magnetization* – transverse to the field axis. It is very small, but non-zero. The magnetic state is demonstrated in Fig. 6. Physically,

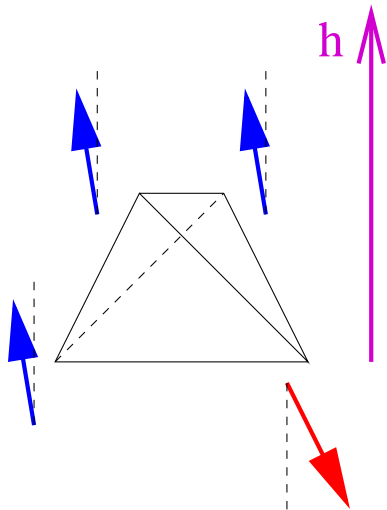


FIG. 6: (Color online) Spin configuration on one tetrahedron for magnetic fields just above the half magnetization plateau.

this would be visible in a single-domain sample as a spontaneously deviation of the magnetization axis from that of the applied field upon leaving the plateau.

The reduced space group symmetry (relative to $Fd\bar{3}m$) of this “canted ferrimagnetic” phase implies that there *must* be at least one phase transition between this state and the fully saturated ferromagnetic state, even at $T > 0$. Moreover, if there is only a single phase transition, a standard Landau analysis – see Appendix A – predicts it cannot be continuous. This is not the case in the BP model, where for small b one observes a single continuous transition into the ferromagnetic state. There are two possibilities: a first order transition from the canted ferrimagnet to the fully polarized state, or an *intermediate phase transition* between the $P4_332$ (R-state structure) canted ferrimagnet and a partially-polarized canted ferromagnet with higher space group symmetry. The latter transition is a possible explanation of the observed magnetization feature at $H \approx 37T$ in HgCr_2O_4 .⁴ Some theoretical aspects of the magnetic behavior near saturation fields have been investigated in Ref.[23].

IV. FURTHER NEIGHBOR INTERACTIONS

In this section we consider how the degeneracy on the plateau might be broken by further neighbor interactions. We take as our model the BP Hamiltonian (Eq.(6)) *plus* additional second and third neighbor exchange interactions:

$$\mathcal{H} = \mathcal{H}_{\text{eff}}^{BP} + J_2 \sum_{\langle\langle ij \rangle\rangle} \mathbf{S}_i \cdot \mathbf{S}_j + J_3 \sum_{\langle\langle\langle k\ell \rangle\rangle\rangle} \mathbf{S}_k \cdot \mathbf{S}_\ell. \quad (18)$$

The corresponding pairs of sites were indicated in Fig.2.

Since the ground states of the BP model are exactly the set of 3:1 collinear states, we may treat the additional small J_2 and J_3 exchange couplings in Eq.(18) as

perturbations. To leading order, this amounts to simply replacing $\mathbf{S}_i = \sigma_i \hat{\mathbf{z}}$ with Ising spins $\sigma_i = \pm 1$ satisfying the 3:1 constraint. Doing so, one obtains *the same effective Ising Hamiltonian* as we found in the spin-lattice model, Eq.(14), but with the effective Ising couplings replaced by the physical second and third neighbor exchanges, $J_{2/3}^{\text{eff}} = J_{2/3}$! Thus it is immediately obvious that if J_2 and J_3 are chosen in a way to match those of the Einstein model (i.e. $J_3 = 2J_2$), the R-state will again be favored.

What state is selected by more general exchange interactions? Consider two adjacent tetrahedra. If the minority spin is at the site joining the two, this is the only configuration the constraint will allow (Fig. 2(a)). Otherwise, two minority sites must be present, in any configuration. This pair can either be next-nearest neighbors (Fig. 2(c)) or 3^{rd} -nearest neighbors (Fig. 2(b)). The latter is preferred when $J_3 > J_2$, and otherwise the former tends to be preferred. This can easily be seen by calculating the total Ising energy of both configurations. The Ising Hamiltonian is satisfied by having *all* pairs of tetrahedra in the preferred (“bent”) generic configuration of the two. This is exactly the same “bending” rule found in the previous section, arising from coupling to lattice distortions. Therefore, the R-state will be the ground state if and only if $J_3 > J_2$. If the opposite relation holds, $J_3 < J_2$, “unbent” configurations are instead favored. This leads to a rather different state with $R\bar{3}m$ symmetry. In this state, the magnetic unit cell is *not* enlarged relative to the non-magnetic one. Instead, all equivalent (i.e. “up” or “down”) tetrahedra have *the same* specific 3:1 configuration. This state is thus directly analogous to the “uud” state expected for a kagome antiferromagnet in a field. It is only 4-fold degenerate (compared to the 8-fold degeneracy of the R-state).

One may also study the further-neighbor exchange model at higher and lower magnetic fields. By straightforward application of the same methods used in Sec.III B, we find that for $J_3 > J_2$, the further-neighbor exchange interactions favor exactly the same canted ferrimagnetic state as the Einstein model just *above* the magnetization plateau (see Fig. 6).

At zero field, the situation is more interesting. Consider a pair of adjacent tetrahedra, as in Fig. 3. This is the smallest cluster of tetrahedra that includes spins interacting via further neighbor exchange. If the coupling b is assumed small relative to J_2, J_3 , and $J_2 > J_3$ then the ground state is collinear, preferring a configuration of parallel spins on a straight line, as opposed to a “bending ice” configuration. The $J_2 < J_3$ case is however more complicated, and the outcome unclear from our limited analysis of a single pair of tetrahedra. Setting $b = 0$, and assuming the magnetization on each tetrahedron vanishes, if $J_2 = J_3$ we find the further neighbor interactions sum to a constant. As a result we can subtract J_2 from J_3 and deal only with the third neighbor interaction terms, with the coefficient $J_3 - J_2 > 0$. Minimizing the third neighbor interaction terms on this single pair

of tetrahedra we find a non-collinear state with a minimum energy of $-\frac{7}{3}(J_3 - J_2)$. The “bending ice” collinear state gives an energy of $-(J_3 - J_2)$, significantly higher. In the non-collinear state, the four spins on each of the two tetrahedra point in four different directions defining a tetrahedron *in spin space*, i.e. with all neighboring pairs of spins at $\approx 109^\circ$ angles to one another. However, we *cannot* tile the entire lattice with this configuration on each pair of tetrahedra. Given the large energy difference between the collinear bending state and the non-collinear state on the single pair, it is reasonable to expect that some other non-collinear state realizes the energy minimum. Of course, as b is increased, collinear states must be favored even at zero field. For sufficiently large b , the ground states for $J_3 > J_2$ are the identical “bending ice” configurations found in the Einstein model.

Other possible interactions in the chromites include dipolar interactions. Spin ice compounds, for example, often have appreciable dipole-dipole interactions²⁴ that cannot be ignored. Using the estimate of the magnetic moment of Cr^{+3} ions in CdCr_2O_4 , $\mu \simeq 3.7\mu_B$ we estimate the dipole-dipole coupling strength to be $D = \frac{\mu_0}{4\pi} \frac{\mu^2}{r_{nn}^3} \simeq 0.3K$ where $r_{nn} = 8.567\text{\AA}$ is the nearest neighbor distance in the CdCr_2O_4 pyrochlore structure. With the experimental observation of the magnetic ordering temperature at a few degrees Kelvin, it is evident that the energy scale of the dominant degeneracy breaking mechanism, regardless of its details, is at least an order of magnitude larger than that of dipolar interactions. For this reason we believe that the dipolar interactions play no significant role in the physics of the chromite spinels, and can be safely neglected.

V. DISCUSSION

In this paper we have studied classical mechanisms of degeneracy breaking in pyrochlore anti-ferromagnets and how this may be related to certain features of the low temperature magnetization curves of the spinel chromites, ZnCr_2O_4 , CdCr_2O_4 , and HgCr_2O_4 . A very simple Einstein phonon model predicts a half-magnetization plateau with a unique ground state spin configuration. Given the known presence of large spin-lattice coupling in these materials,^{4,5} this seems the most likely explanation of the plateau state. Neutron scattering measurement of the R-state structure on the plateau in any of these materials would provide good support of this proposal.

Nevertheless, the same ground state *could* in principle be stabilized by other sorts of interactions. For instance, as we have shown, further neighbor exchange with $J_3 > J_2$ would also lead to the R-state. This relation amongst exchanges seems contrary to simple expectations that antiferromagnetic superexchange decays with distance. However, the exchange paths for these two interactions (and indeed some further-neighbor exchanges) are quite similar (see Ref.25), so one should have an open

mind to this possibility. It would thus be desirable to have an independent comparison of the two theoretical models.

One further check on the Einstein model would be to consider its predictions in zero field. As we have seen, despite the selection of a unique ground state on the plateau, in zero field the Einstein model continues to predict a large degeneracy of states. In reality, of course, this degeneracy will be broken by further interactions (e.g more complex phonons, further-neighbor exchange, Dzyaloshinskii-Moriya interactions) beyond the Einstein model. Interestingly, the zero field ordered phases for ZnCr_2O_4 , CdCr_2O_4 , and HgCr_2O_4 are known from neutron scattering and are known to be *different*.^{6,7,26} This is indeed consistent with the Einstein model in the sense that the further very small interactions beyond the model would be expected to select different states in each material. Interestingly, the Einstein model suggests that despite this panoply of phases at zero field, all these materials may display a *universal* ordering on their magnetization plateau: the R-state structure.¹⁵

As we have seen in Sec.IV, under some circumstances ($J_3 > J_2$ and b not too large), the further-neighbor exchange model may have a non-collinear ground state. This would be clearly distinguishable from the collinear states preferred by the spin-lattice interactions. For instance, Goldstone’s theorem implies that a collinear ground state in zero field will have two gapless spin wave modes, while a non-collinear state will have *three*. However, we caution that additional effects beyond the Einstein model, especially Dzyaloshinskii-Moriya interactions, could induce some small non-collinearity even if the predominant interactions are of the spin-lattice type.

Another general prediction of the Einstein phonon model is that the interactions (b) which stabilize the plateau are *of the same order* as those (b') which select the ordered R-state out of all possible plateau configurations. This has physical consequences. Specifically, the energy cost of a spin excitation which leads to a deviation from the quantized plateau magnetization is expected to be of the same order as a spinless excitation which re-arranges the 3:1 configurations but leaves the magnetization unchanged. On heating the sample, the former excitations are responsible for the rounding of the plateau, while the latter are responsible for the destruction of the R-state magnetic order, i.e the restoration of the spinel space group symmetry. Because both excitations will be excited roughly equally, we expect that the thermal phase transition from the R-state to the high-temperature phase should occur at a critical temperature T_c which is of the same order of magnitude as the scale at which the plateau forms, and the 3:1 constraint itself is rather strongly violated.

Because the 3:1 constraint is not significant at this temperature, a conventional Landau-Ginzburg-Wilson analysis of this critical point is valid (see Ref.[16] for a discussion of the alternative scenario which would apply if $T_c \ll T_p$, where T_p is the temperature at which the

plateau forms). The result of such an analysis – detailed in Appendix A – is that the thermal transition should be *first order*. This is in agreement with experimental findings.

There are many open directions for future work. An important one is to understand more microscopically the mechanisms of exchange interactions and spin-lattice coupling. Goodenough-Kanamori analysis actually predicts a competition between two processes effecting the nearest neighbor exchange interaction: antiferromagnetic *direct* Cr-Cr exchange, and ferromagnetic Cr-X-Cr superexchange in the ideal crystal structure, because of 90° Cr-X-Cr (X=O,S,Se) bonds.²⁵ The angle of the Cr-X-Cr bonds is generally not exactly 90° however, and is affected by the u -parameter in the spinel structure. The prevailing belief is that the competition of these two processes is most strongly effected by the overall expansion/contraction of the lattice, but the different u -parameters in different materials may also be important. Longer distance super-exchange processes between second, third, and fourth neighbor pyrochlore sites involve comparable exchange paths, and their relative magnitudes are not presently clear. Turning to spin-lattice coupling, an interesting speculation is that the important phonon modes are those which modify the Cr-X-Cr angles, thus strongly affecting the nearest-neighbor superexchange contribution. This is an appealing possibility given the observation of changes between ferromagnetic and antiferromagnetic behavior in small changes of temperature and field in HgCr_2S_4 .²⁷ A broader understanding of the microscopic mechanisms of spin and spin-lattice interactions in these materials would be of considerable interest even beyond the realm of frustrated magnetism.

In summary, the study here clearly highlights the sensitivity of the magnetic state in antiferromagnetic pyrochlores to further microscopic interactions. A simple Einstein model makes the prediction that the R-state order should be observed in many materials and we hope that detailed neutron scattering studies will be forthcoming to test this prediction.

Acknowledgments

We are grateful to H. Ueda, Y. Motome, M. Matsuda, H. Takagi, and Y. Ueda for discussions, and to H. Ueda, H. Mitamura, T. Goto, and H. Takagi for sharing their experimental data with us prior to publication. We also wish to acknowledge fruitful discussions with S. Trebst regarding some of the numerical work presented in this paper. This work was supported by NSF Grant DMR04-57440, PHY99-07949, and the Packard Foundation.

APPENDIX A: LANDAU-GINZBURG THEORY FOR THE FINITE TEMPERATURE TRANSITION OUT OF THE PLATEAU STATE

In the R-state¹⁵ the enlarged spin periodicity, including 4 unit cells of the underlying pyrochlore lattice, manifests itself in the appearance of non-zero Fourier components with a momentum vector not at the Γ point in the Brillouin Zone (BZ). These Fourier components therefore serve as order parameters for the R-state. Then, using these order parameters and their transformation under the various lattice symmetries, we can construct a Landau-Ginzburg theory to determine whether a finite temperature transition out of this ordered state should be 1st order or 2nd order, at least at the mean field level.

Previous work by some of the authors¹⁶ has encountered the same R-state in a different formulation, using a PSG (Projective Symmetry Group) analysis. We find the Fourier components are at the 3 momentum vectors $\mathbf{k}_1 = \frac{1}{a}(\pi, 0, 0)$, $\mathbf{k}_2 = \frac{1}{a}(0, \pi, 0)$, and $\mathbf{k}_3 = \frac{1}{a}(0, 0, \pi)$. These form a k-star of the point symmetry group of the lattice. This particular k-star has only 6-dimensional irreps (irreducible representations) of the point symmetry group. Therefore the order parameter can be cast as a 6-component real vector. These components can be understood as degrees of freedom equivalent to the real and imaginary parts of the 3 Fourier components.

The R-state corresponds to 8 configurations of this more general order parameter $\vec{v} = (\sigma_1, \sigma_2, \sigma_3, 0, 0, 0)v$ or $\vec{v} = (0, 0, 0, \sigma_4, \sigma_5, \sigma_6)v$ where $\sigma_j = \pm 1$, and we allow only the 8 cases where $\sigma_1\sigma_2\sigma_3 = +1$ or $\sigma_4\sigma_5\sigma_6 = +1$.

This order parameter was derived using the PSG analysis. However, it is possible to derive this order parameter more directly, by finding the “density” of minority sites $\rho_j = \frac{1}{2}(1 - S_j^z)$. A straightforward Fourier analysis results in

$$\begin{aligned} \rho(x, y, z) = & \\ & \frac{1}{4} \left(1 + \sigma_4 \sqrt{2} \cos \frac{\pi}{a} x + \sigma_5 \sqrt{2} \cos \frac{\pi}{a} y + \sigma_6 \sqrt{2} \cos \frac{\pi}{a} z \right. \\ & \left. - \sigma_1 \sqrt{2} \sin \frac{\pi}{a} x - \sigma_2 \sqrt{2} \sin \frac{\pi}{a} y - \sigma_3 \sqrt{2} \sin \frac{\pi}{a} z \right), \end{aligned} \quad (\text{A1})$$

where (x, y, z) are the real space coordinates of the pyrochlore lattice sites.

In this representation we construct invariants (or Casimir operators) from the 6 components $\{v_j\}_{j=1}^6$ of \vec{v} . The Landau-Ginzburg (LG) theory is then constructed out of all these invariants. In this way we find the most general LG free energy allowed by the symmetry of the

lattice

$$\begin{aligned}
F = & m\bar{v}^2 + \gamma (v_1v_2v_3 + v_4v_5v_6) + u_1\bar{v}^4 \\
& + u_2 \sum_{j=1}^3 v_j^2 \sum_{i=4}^6 v_i^2 \\
& + u_3 \left[\sum_{i \neq j=1}^3 (v_i v_j)^2 + \text{other trio} \right].
\end{aligned} \tag{A2}$$

The 8 R-state configurations are favored for a part of the coupling space $\gamma < 0$, $m < 0$, $u_1 > 0$, $u_2 > 0$, and $u_3 < 0$.

The transition into the orderless state is tuned by m changing sign. We take $\bar{v} = (1, 1, 1, 0, 0, 0)v$ without loss of generality, and simplify the free energy to a single variable function

$$F(v) = m'v^2 - |\gamma|v^3 + |u'|v^4. \tag{A3}$$

Due to the cubic term, the transition is predicted by MFT to be 1st order.

APPENDIX B: PROOF OF BENDING RULE INDUCING THE R-STATE

In this appendix we explain how from the ‘‘bending’’ rule for the 3 : 1 configurations, we can construct only the R state.

Consider the unit cell of the R state, including 4 up pointing tetrahedra as in Fig. 1. We will show that using bending configurations on pairs of tetrahedra, we will find a unique state (up to lattice symmetries).

We start by picking a pair of tetrahedra to be in the bending configuration. We can then pick the unit cell orientation such that it matches the placements of the minority sites in Fig. 7(a) - the two adjacent tetrahedra share site 1 and the two minority sites are 2 and 6.

Next we consider the tetrahedron pairs sharing sites 3 and 5, shown in Fig. 7(b). For the pair sharing site 3, we can pick sites 4 or 7 to be minority sites. Similarly, for the pair sharing site 5, we can pick sites 4 or 8 to be minority sites. We cannot pick 4 and 7 or 4 and 8, since then we will have nearest neighbor minority sites. We also cannot pick 7 and 8, since then the pair of tetrahedra sharing site 4 will *not* be in a bending configuration - sites 7,4 and 8 sit on a straight line. We must therefore choose site 4 to be a minority site, (see Fig. 7(c)). Already a tendency to form flippable plaquettes is evident.

Now we turn to the upper layer of tetrahedra (the tetrahedra outlined by dashed lines). Considering the pair of tetrahedra adjoined at site 7, we conclude that site

9 *cannot* be a minority site. Similar considerations deem sites 10 and 11 cannot be minority sites. This should be most clearly evident from the 3-fold rotational symmetry of the minority site configuration about an axis perpendicular to the paper. We mark these sites in Fig. 7(d) by a full gray circle.

The pair of tetrahedra sharing site 7 can allow a minority site on either site 12 or 13. If we choose site 13 (as in Fig. 7(e)), then now we cannot choose site 14 to be a minority site, as it neighbors site 13, and we also cannot choose site 15 to be a minority site, as 13,14 and 15 sit on a straight line. Now considering the pair of tetrahedra sharing site 16, we reach an impasse - the tetrahedron of sites 11, 14, 15 and 16 cannot have a minority site on any one of its corners! Therefore, we *cannot* choose site 13 to be a minority site, we can only choose site 12!

Due to the 3-fold rotation symmetry of the spin structure we have layed out so far the same argument applies to all three down pointing tetrahedra in the upper (dashed) layer. The single up pointing tetrahedron must therefore have a minority site located at site 17. The resulting configuration, shown in Fig. 7(f) is the unit cell of the R-state.

Next we demonstrate that the R state is the only 3 : 1 spin configuration that can be constructed from these cell structures. We can add the minority site positions on the remaining tetrahedra in the cell cluster, as shown in Fig. 8(a). Each cell has 4 hexagonal plaquettes. One is ‘‘flippable’’ - alternating between majority and minority sites. The other three plaquettes have one minority site, and 5 majority sites. There is only one way to attach an identical cell with the flippable plaquette, but apriori there are three ways to attach two cells through a plaquette with only 1 minority site (we have the freedom to choose which one of the other 3 plaquettes of the second cell is the flippable one).

Consider the cell sharing the hexagonal plaquette that involves sites 1, 6, 16 and 14. Since sites 6 and 15 are already set to be minority sites, the flippable plaquette in this cell *must* be the one going through sites 6, 16 and 15, marked by purple lines. We therefore do *not* have three choices of how to place the minority sites on this cell, but rather only one. The whole cluster, with the given spin configuration, still retains a 3-fold rotational symmetry about an axis perpendicular to the paper. We use this symmetry to deduce that the same considerations apply to the other three plaquettes with one minority site, and there is no freedom in how to choose the spin configurations in *all* the surrounding cells. Therefore, there can only be one way to arrange the minority sites with the given cell, and that is the R-state configuration.

¹ K. Penc, N. Shannon, and H. Shiba, Phys. Rev. Lett. **93**, 197203 (2004).

² R. Moessner, Can. J. Phys. **79**, 1283 (2001).

³ R. Moessner and J. Chalker, Phys. Rev. B **58**, 12049 (1998).

⁴ H. Ueda, H. Mitamura, T. Goto, and H. Takagi, Phys. Rev.

- B **73**, 094415 (2006).
- ⁵ H. Ueda, H. A. Katori, H. Mitamura, T. Goto, and H. Takagi, *Phys. Rev. Lett.* **94**, 047202 (2005).
 - ⁶ S.-H. Lee, C. Broholm, W. Ratcliff, G. Gasparovic, Q. Huang, T. H. Kim, and S.-W. Cheong, *Nature* **418**, 856 (2002).
 - ⁷ J. H. Chung, M. Matsuda, S. H. Lee, K. Kakurai, H. Ueda, T. J. Sato, H. Takagi, K. P. Hong, and S. Park (2005).
 - ⁸ U. Hizi and C. L. Henley, *Phys. Rev. B* **73**, 054403 (2006).
 - ⁹ C. L. Henley, *Phys. Rev. Lett.* **96**, 047201 (2006).
 - ¹⁰ U. Hizi, P. Sharma, and C. L. Henley, *Phys. Rev. Lett.* **95**, 167203 (2005).
 - ¹¹ M. Elhajal, B. Canals, R. Sunyer, and C. Lacroix, *Phys. Rev. B* **71**, 094420 (2005).
 - ¹² A. Koga and N. Kawakami, *Phys. Rev. B* **63**, 144432 (2001).
 - ¹³ A. B. Harris, A. J. Berlinsky, and C. Bruder, *J. Appl. Phys.* **69**, 5200 (1991).
 - ¹⁴ H. Tsunetsugu, *Phys. Rev. B* **65**, 024415 (2001).
 - ¹⁵ D. L. Bergman, R. Shindou, G. A. Fiete, and L. Balents, *Phys. Rev. Lett.* **96**, 097207 (2006).
 - ¹⁶ D. L. Bergman, G. A. Fiete, and L. Balents, *Phys. Rev. B* **73**, 134402 (2006).
 - ¹⁷ D. L. Bergman, R. Shindou, G. A. Fiete, and L. Balents, in preperation.
 - ¹⁸ C. Jia, J. H. Nam, J. S. Kim, and J. H. Han, *Phys. Rev. B* **71**, 212406 (2005).
 - ¹⁹ See R. P. Van Staple in *Ferromagnetic Materials* vol 3, ed. E. P. Wohlfarth (Amsterdam: North-Holland)1982 pg 603 and references therein. See also A. Selmi, A. Mauger, and M. Heritier, *J. Phys. C* **18**, 5599 (1985); F. K. Lotgering, in *Proceedings of the International Conference on Magnetism*, Nottingham, 1964 (Institute of Physics and the Physical Society, London, 1965), p. 533; J. M. Hastings and L. M. Corliss, *J. Phys. Chem. Solids* **29**, 9 (1968); R. Plumier, *J. Appl. Phys.* **37**, 964 (1966).
 - ²⁰ O. Tchernyshyov, R. Moessner, and S. L. Sondhi, *Phys. Rev. B* **66**, 064403 (2002).
 - ²¹ D. G. Wickham and J. B. Goodenough, *Phys. Rev.* **115**, 1156 (1959).
 - ²² Y. Motome, K. Penc, and N. Shannon, *J. Mag. Mag. Mater.* **300**, 57 (2006).
 - ²³ O. Derzkho and J. Richter, *Phys. Rev. B* **72**, 094437 (2005).
 - ²⁴ S. T. Bramwell and M. J. P. Gingras, *Science* **294**, 1495 (2001).
 - ²⁵ P. K. Baltzer, P. J. Wojtowicz, M. Robbins, and E. Lopatin, *Phys. Rev.* **151**, 367 (1966).
 - ²⁶ S.-H. Lee, C. Broholm, T. H. Kim, W. Ratcliff, and S.-W. Cheong, *Phys. Rev. Lett.* **84**, 3718 (2000).
 - ²⁷ V. Tsurkan, J. Hemberger, A. Krimmel, H.-A. K. von Nidda, P. Lunkenheimer, S. Weber, V. Zestrea, and A. Loidl, Unpublished, cond-mat/0603348.

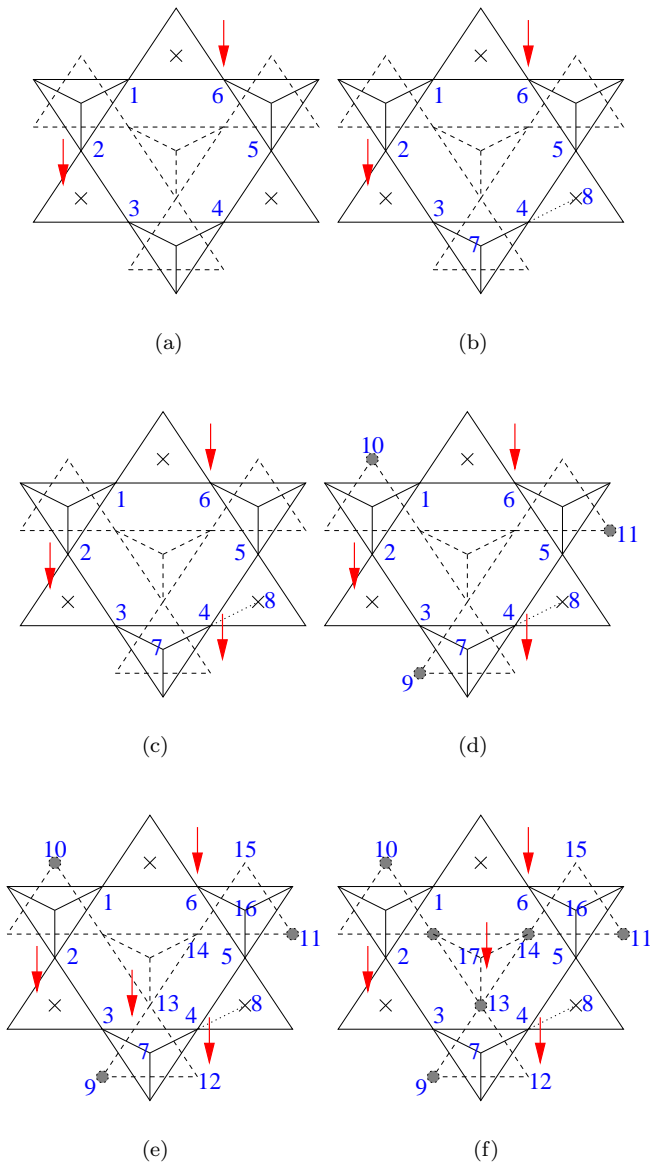
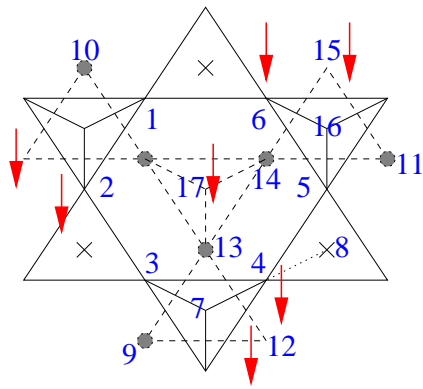
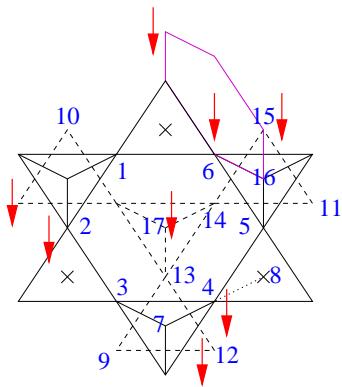


FIG. 7: (Color online) Stages in the graphical proof that the bending rule allows only the R state to form with the 3 : 1 constraint. The down pointing triangles, with lines joining at their centers, represent tetrahedra pointing out of the plane of the paper, with the center point representing the upper corner. The up pointing triangles in the figures represent tetrahedra pointing into the paper, with the lowest corner being represented by the center position (sometimes marked by a small cross). The dashed lines represent an upper layer of tetrahedra, above the solid line tetrahedra. It is instructive to contrast this projection with Fig. 1 - both show the *same* cluster of tetrahedra. To avoid clutter, we mark only the minority sites, by down pointing (red) arrows. We mark sites that we conclude are not allowed to be minority sites by a full gray circle.



(a)



(b)

FIG. 8: (Color online) Stages in the graphical proof that the bending rule allows only the R state to form with the 3 : 1 constraint. The down pointing triangles, with lines joining at their centers, represent tetrahedra pointing out of the plane of the paper, with the center point representing the upper corner. The up pointing triangles in the figures represent tetrahedra pointing into the paper, with the lowest corner being represented by the center position (sometimes marked by a small cross). The dashed lines represent an upper layer of tetrahedra, above the solid line tetrahedra. It is instructive to contrast this projection with Fig. 1 - both show the *same* cluster of tetrahedra. To avoid clutter, we mark only the minority sites, by down pointing (red) arrows. We mark sites that we conclude are not allowed to be minority sites by a full gray circle.